EPJ Web of Conferences **364**, 11007 (2026) https://doi.org/10.1051/epjconf/202636411007
Quark Matter 2025

Strangeness production in different collision systems and at different collision energies with the STAR experiment

Weiguang Yuan[1,*] for the STAR Collaboration

[1]Tsinghua University, Beijing 100084, China

Abstract.
Strangeness production has been suggested as a sensitive probe to the early dynamics of the deconfined matter created in heavy-ion collisions. In these proceedings, we report new measurements of strange hadron (K^0_s, Λ, $\bar{\Lambda}$, Ξ, $\bar{\Xi}$, ϕ, Ω, $\bar{\Omega}$) production in Au+Au collisions at $\sqrt{s_{NN}}$ = 7.7, 9.2, 11.5, 14.6, 19.6 GeV and in O+O, Zr+Zr and Ru+Ru collisions at $\sqrt{s_{NN}}$ = 200 GeV. The presented results include transverse momentum spectra, rapidity distributions, nuclear modification factors ($R_{\rm CP}$), antibaryon-to-baryon ratio, and Ω-to-ϕ ratios. A significant Ω-to-ϕ enhancement is observed in central Au+Au collisions at $\sqrt{s_{NN}} \geq 7.7$ GeV, with a similar trend in O+O and isobar (Zr+Zr, Ru+Ru) collisions at 200 GeV, where the enhancement grows from peripheral to central events. The results hint at a possible Ω-to-ϕ enhancement pattern that appears consistent at similar N_{part} values across different collision systems at $\sqrt{s_{NN}}$ = 200 GeV.

1 Introduction

Strange hadrons serve as sensitive and versatile probes of heavy-ion collisions dynamics. The enhanced production of total strange hadron yields (dominated by the low p_T yields) relative to p+p collisions was initially proposed as a signature of quark-gluon plasma (QGP) formation [1]. Recent studies have demonstrated that these yields can be well described by statistical models and used to extract chemical freeze-out parameters [2]. At intermediate p_T, hyperon-to-meson enhancement may arise from hadronization via parton coalescence/recombination [3], while nuclear modification factors at high p_T reflect partonic energy loss in the medium.

Strange hadron production in Au+Au collisions exhibits a strong energy dependence, which have been explored systematically in the Beam Energy Scan (BES) programs at STAR. In BES-I, the nuclear modification factors ($R_{\rm CP}$) of strange hadrons showed energy-dependent behaviors [4], while the Ω/ϕ ratios displayed clear enhancement at higher energies but remained ambiguous at lower energies [5]. Strangeness and baryon chemical potentials (μ_S and μ_B) at chemical freeze-out temperature ($T_{\rm ch}$) have been extracted from yield ratios and compared with lattice QCD predictions [6]. The higher-precision BES-II data will not only further constrain these parameters but also clarify the disappearance of QGP signatures at lower energies.

The system size required for QGP formation remains a key open question. STAR has studied strange hadron yield ratios (Λ/π, Ξ/π, Ω/π) across p+p, Cu+Cu and Au+Au collisions [7–10], but measurements in low-multiplicity systems remain sparse. Additionally, comprehensive studies of $R_{\rm cp}$ and Ω/ϕ ratios across different collision systems are lacking

*e-mail: ywg24@mails.tsinghua.edu.cn

[3, 11]. With new high-statistics data from d+Au, O+O and isobar (Ru+Ru, Zr+Zr) collisions at $\sqrt{s_{NN}}$ = 200 GeV, The evolution of dynamics with system size can be systematically probed by STAR, particularly in the small-system regime.

2 Experiment and analysis details

The datasets analyzed in these studies include Au+Au collisions at $\sqrt{s_{NN}}$ = 7.7–19.6 GeV and O+O, Zr+Zr, and Ru+Ru collisions at $\sqrt{s_{NN}}$ = 200 GeV, recorded by the STAR detector during the 2018–2021 runs. The STAR detector provides large, uniform acceptance and excellent particle identification capabilities, primarily utilizing the Time Projection Chamber (TPC) and the Barrel Time-of-Flight Detector (BTOF). The upgraded inner TPC (iTPC) extends pseudorapidity coverage from $|\eta| < 1.0$ to $|\eta| < 1.5$ and improves low-momentum acceptance by reducing the p_T threshold from 100 MeV/c to 60 MeV/c. Strange hadrons (K^0_S, $\Lambda/\bar{\Lambda}$, $\Xi^-/\bar{\Xi}^+$, $\Omega^-/\bar{\Omega}^+$) are reconstructed via their decay topologies using daughter tracks ($\pi^\pm$, $K^\pm$, $p/\bar{p}$). The ϕ meson, due to its short lifetime, is treated as originating from the primary vertex. The identification of $K^\pm$ for ϕ meson reconstruction is achieved by combining ionization energy loss (dE/dx) measurements from the TPC with time-of-flight information from the BTOF. For other strange particles, only the TPC dE/dx information is utilized. The high statistics of reconstructed strange hadrons enable detailed multi-differential measurements across collision systems and energies.

3 Results and Discussion

3.1 Rapidity spectra

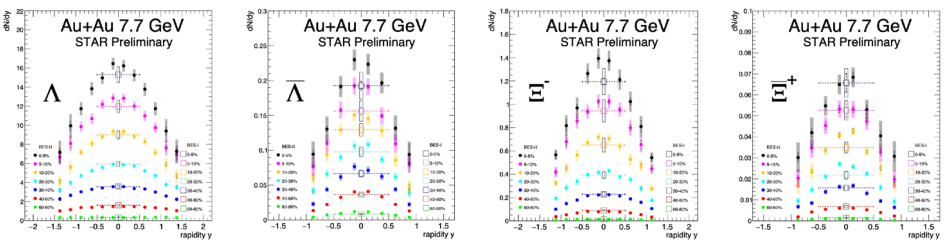

Figure 1. The rapidity spectra of $\Lambda(\bar{\Lambda})$ and $\Xi^-(\bar{\Xi}^+)$ in Au + Au collisions at $\sqrt{s_{NN}}$ = 7.7 GeV, for different centrality ranges. The systematic errors are shown as colored boxes, while the statistical errors are shown as vertical lines. The solid points are from BES-II data while the open points are published results from BES-I [4].

The p_T spectra of strange hadrons are determined by efficiency-correcting the raw yields extracted from invariant mass distributions within well-defined mass windows. For $\Lambda(\bar{\Lambda})$, $\Xi^-(\bar{\Xi}^+)$, $\Omega^-(\bar{\Omega}^+)$, and ϕ, we obtain the full p_T-integrated yields (dN/dy) as functions of rapidity through extrapolation of the measured p_T spectra. The high-statistics STAR dataset enables precise measurement of rapidity distributions in fine $\Delta y = 0.25$ bins.

Figure 1 presents the rapidity spectra of Λ, $\bar{\Lambda}$, Ξ^-, and $\bar{\Xi}^+$ at $\sqrt{s_{NN}}$ = 7.7 GeV, highlighting the extended acceptance of the iTPC upgrade. The preliminary BES-II results (solid symbols) agree with published BES-I data (open symbols) [4] within uncertainties.

The rapidity spectra reveal distinct baryon/anti-baryon differences: while anti-baryon distributions ($\bar{\Lambda}$, $\bar{\Xi}^+$) are approximately Gaussian, the baryon spectra (Λ, Ξ^-) exhibit significantly broader distributions. This broadening arises primarily from contributions of stopped baryons, consistent with previous observations by the NA49 collaboration [12].

3.2 Nuclear modification factor from $\sqrt{s_{NN}}$ = 7.7 to 19.6 GeV

Figure 2 shows the nuclear modification factor, $R_{\rm CP}$ of $K^0_S, \phi, \Lambda(\bar{\Lambda}), \Xi^-(\bar{\Xi}^+)$ in Au+Au collisions from $\sqrt{s_{NN}}$ = 7.7 to 19.6 GeV. The definition of $R_{\rm CP}$ is the ratio of particle yield in central collisions to that in peripheral collisions, both of which are scaled by the average number of inelastic binary collisions $\langle N_{\rm coll} \rangle$,

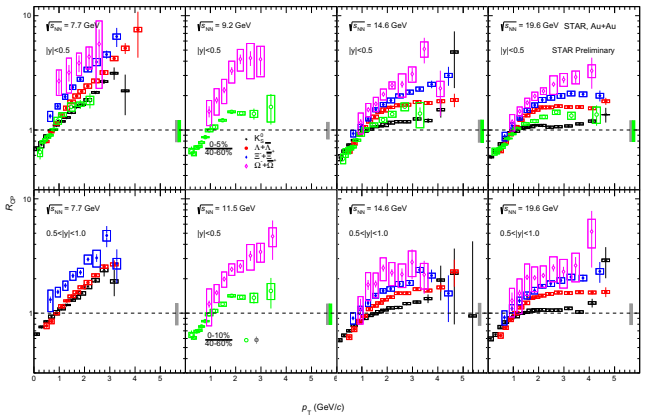

Figure 2. K^0_S, $\Lambda+\bar{\Lambda}$, $\Xi^-+\bar{\Xi}^+$ R_{CP} (0-5%)/(40-60%), at midrapidity (|y| < 0.5) and larger rapidity (0.5 < |y| < 1.0) in Au + Au collisions from $\sqrt{s_{NN}}$ = 7.7 to 19.6 GeV. The vertical bars represent the statistical errors and the box on those data points of K^0_S, Λ, Ξ represent the systematic errors.

$$R_{\rm CP} = \frac{\left[(dN/dp_T)\,/\,\langle N_{\rm coll}\rangle\right]_{\rm central}}{\left[(dN/dp_T)\,/\,\langle N_{\rm coll}\rangle\right]_{\rm peripheral}} \tag{1}$$

The nuclear modification factor $R_{\rm CP}$ would equal unity if nucleus-nucleus collisions were simply superpositions of nucleon-nucleon collisions. However, the $R_{\rm CP}$ for nearly all strange particles remain consistently above unity at high p_T across $\sqrt{s_{NN}}$ = 7.7 to 19.6 GeV. As shown in Fig. 2, there are distinct energy-dependent behaviors: for $\sqrt{s_{NN}} \geq$ 14.6 GeV, $R_{\rm CP}$ approaches a constant value above unity at $p_T >$ 2 GeV/c, while at lower energies ($\sqrt{s_{NN}} \leq$ 11.5 GeV) it exhibits a continuous rise with increasing p_T. The observed enhancement in this intermediate-p_T region likely stems from a combined effect of radial flow and the growing dominance of quark coalescence over fragmentation during hadronization. This enhancement exhibits a clear hierarchy, being more pronounced for Ω and Ξ than for Λ and K^0_S. Furthermore, The $R_{\rm CP}$ at mid-rapidity (|y| < 0.5) remains comparable to that at larger rapidity (0.5 < |y| < 1.0), suggesting minimal rapidity dependence.

3.3 Ω/ϕ ratio in Au+Au collisions from $\sqrt{s_{NN}}$ = 7.7 to 19.6 GeV and in isobar and O+O collisions at $\sqrt{s_{NN}}$ = 200 GeV

Figures 3 presents the Ω/ϕ ratio measured in Au+Au collisions at $\sqrt{s_{NN}}$ = 7.7-19.6 GeV, Fig. 4 shows the ratio in isobar (Ru+Ru, Zr+Zr) and O+O collisions at $\sqrt{s_{NN}}$ = 200 GeV, across several centrality bins (0-5%, 20-30%, 40-60%, and 60-80%). A significant enhancement of the Ω/ϕ ratio is observed at intermediate p_T in central Au+Au collisions throughout the studied energy range, likely driven by the combined effects of radial flow and quark coalescence mechanism. Notably, within each centrality bin (0-10%, 20-30%, and 40-60%), the Ω/ϕ ratios remain consistent across all collision energies from 7.7 to 19.6 GeV within experimental uncertainties.

The analysis of smaller collision systems reveals similar enhancement patterns: in both isobar and O+O collisions, the Ω/ϕ ratio shows significant enhancement relative to p+p collisions, with a clear centrality dependence - increasing from peripheral to central collisions. The enhancement is more pronounced in central isobar collisions compared to central O+O collisions. More importantly, comparing systems with similar participant numbers (N_{part}) indicate that there is no significant system size dependence in the Ω/ϕ ratio: the ratio in central O+O collisions matches that in 40-60% isobar collisions, while the 20-30% O+O results agree with 60-80% isobar collisions. This consistency suggests that the enhancement mechanism is primarily governed by the N_{part} rather than the collision species at $\sqrt{s_{NN}}$ = 200 GeV.

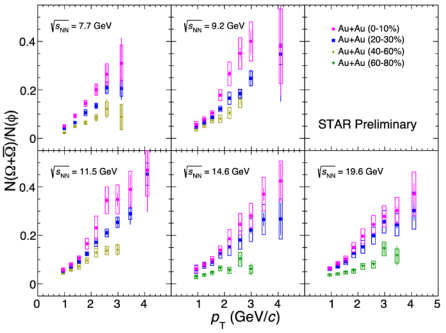

Figure 3. Ω/ϕ ratio in Au + Au collisions from $\sqrt{s_{NN}}$ = 7.7 to 19.6 GeV in the centralities of 0–10%, 20–30%, 40-60% and 60–80%. The systematic errors are shown as colored boxes, while the statistical errors are shown as vertical lines.

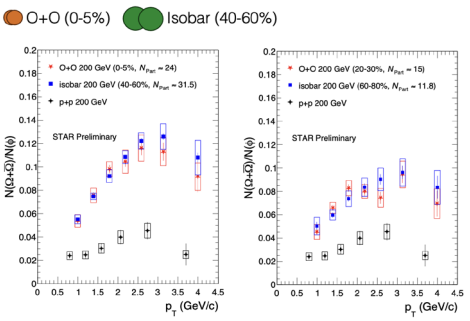

Figure 4. Ω/ϕ ratio in isobar and O+O collisions at $\sqrt{s_{NN}}$ = 200 GeV in the centralities of 0–5%, 20–30%, 40-60% and 60–80%. The systematic errors are shown as colored boxes, while the statistical errors are shown as vertical lines.

4 Summary

In these proceedings, we present new STAR measurements of strangeness production in heavy-ion collisions, analyzing Au+Au collisions from the BES-II program ($\sqrt{s_{NN}}$ = 7.7-19.6 GeV) along with O+O and isobar (Ru+Ru/Zr+Zr) systems at $\sqrt{s_{NN}}$ = 200 GeV. The data reveal three significant observations. Firstly, baryons (Λ, Ξ^-) show broader rapidity distributions than their antibaryon counterparts ($\bar{\Lambda}, \bar{\Xi}^+$), that arises from stopped baryon contributions at $\sqrt{s_{NN}}$ = 7.7 to 19.6 GeV. Secondly, central Au+Au collisions exhibit strong Ω/ϕ enhancement at intermediate p_T throughout the BES-II energy range, suggesting combined effects from quark coalescence and radial flow. Thirdly, when comparing systems with similar N_{part}, such as central O+O versus mid-central (40-60%) isobar collisions, the Ω/ϕ enhancement shows no significant dependence on collision species, suggesting the phenomenon is primarily governed by N_{part}. These comprehensive measurements, with extended p_T and rapidity coverage, provide new insights into strangeness production mechanisms across different collision systems and energies.

References

[1] J. Chen *et al.* Nucl. Sci. Tech. **35**, no.12, 214 (2024)
[2] L. Adamczyk *et al.* [STAR], Phys. Rev. C **96**, no.4, 044904 (2017)
[3] B. I. Abelev *et al.* [STAR], Phys. Rev. Lett. **99**, 112301 (2007)
[4] J. Adam *et al.* [STAR], Phys. Rev. C **102**, no.3, 034909 (2020)
[5] L. Adamczyk *et al.* [STAR], Phys. Rev. C **93**, no.2, 021903 (2016)
[6] D. Bollweg *et al.* Phys. Rev. D **110**, no.5, 5 (2024)
[7] B. I. Abelev *et al.* [STAR], Phys. Rev. C **75**, 064901 (2007)
[8] G. Agakishiev *et al.* [STAR], Phys. Rev. Lett. **108**, 072301 (2012)
[9] B. I. Abelev *et al.* [STAR], Phys. Rev. C **79**, 034909 (2009)
[10] M. M. Aggarwal *et al.* [STAR], Phys. Rev. C **83**, 034910 (2011)
[11] J. Adams *et al.* [STAR], Phys. Rev. Lett. **98**, 062301 (2007)
[12] C. Alt *et al.* [NA49], Phys. Rev. C **78**, 034918 (2008)